Frequency- and Time-Domain FEM Models of EMG: Capacitive Effects and Aspects of Dispersion

Nikolay S. Stoykov*, *Member, IEEE*, Madeleine M. Lowery, *Member, IEEE*, Allen Taflove, *Fellow, IEEE*, and Todd A. Kuiken, *Member, IEEE*

Abstract—**Electromyography (EMG) simulations have traditionally been based on purely resistive models, in which capacitive effects are assumed to be negligible. Recent experimental studies suggest these assumptions may not be valid for muscle tissue. Furthermore, both muscle conductivity and permittivity are frequency-dependent (dispersive). In this paper, frequency-domain and time-domain finite-element models are used to examine the impact of capacitive effects and dispersion on the surface potential of a volume conductor. The results indicate that the effect of muscle capacitance and dispersion varies dramatically. Choosing low conductivity and high permittivity values in the range of experimentally reported data for muscle can cause displacement currents that are larger than conduction currents with corresponding reduction in surface potential of up to 50% at 100 Hz. Conductivity and permittivity values lying toward the middle of the reported range yield results which do not differ notably from purely resistive models. Also, excluding dispersion can also cause large error—up to 75% in the high frequency range of the EMG. It is clear that there is a need to establish accurate values of both conductivity and permittivity for human muscle tissue *in vivo* in order to quantify the influence of capacitance and dispersion on the EMG signal.**

Index Terms—**EMG, finite-element methods.**

I. INTRODUCTION

TO DATE, models in electromyography (EMG) have been based on an assumption of quasi-stationarity at the macroscopic level. Purely resistive electric properties have been assigned to all tissues [9], [15], [3]. Capacitive properties have been introduced only at the microscopic level with respect to the cell membrane [35]. In the closely related field of electrical stimulation, the capacitance of the cell membrane has been considered in the derivation of the activation function and in the study of its properties [27]–[29], [25]. The tissue surrounding

*N. S. Stoykov is with the Rehabilitation Institute of Chicago, IL 60611 USA and with the Department of Physical Medicine and Rehabilitation, Northwestern University, Chicago, IL 60611 USA (e-mail: n-stoykov@northwestern.edu).

M. M. Lowery is with the Rehabilitation Institute of Chicago, IL 60611 USA and with the Department of Physical Medicine and Rehabilitation, Northwestern University, Chicago, IL 60611 USA.

A. Taflove is with the Department of Electrical and Computer Engineering, Northwestern University, Evanston, IL 60208 USA.

T. A. Kuiken is with the Rehabilitation Institute of Chicago, IL 60611 USA, with the Department of Physical Medicine and Rehabilitation, Northwestern University, Chicago, IL 60611 USA and with the Department of Electrical and Computer Engineering, Northwestern University, Evanston, IL 60208 USA.

the activated fiber is assumed to be purely resistive. In addition, macroscopic cardiothoracic models for defibrillation [5], [18] and for magnetic stimulation [2] have been based on the same assumption. Capacitive properties have also been considered and deemed negligible in a model of magnetic stimulation of the brain cortex [6]. They have been included in a high-frequency bio-electromagnetic model for calculating electromagnetic absorption in humans in the 100–350 MHz range [33]. And finally, they have been used in models of electrical impedance tomography at 28.8 kHz [8] and in the 2–200 kHz range [16].

The condition for neglecting capacitive effects in homogeneous bio-electromagnetic models, has been described by Plonsey and Hepner [26], as follows:

$$\frac{\omega \varepsilon_0 \varepsilon_r}{\sigma} \ll 1 \tag{1}$$

where σ and ε_r denote the conductivity and the relative permittivity of the tissue, and ω the angular frequency of the source. $\varepsilon_0 = 8.854 \times 10^{-12}$ F/m is the permittivity of vacuum. The results of recent experimental studies, however, suggest that (1) may not be valid for muscle tissue [12], [14]. It is unclear how capacitive effects may alter the amplitude, frequency content, and phase distribution of EMG signals detected throughout the muscle and at the skin surface.

It is apparent from (1) that the magnitude of the capacitive effects depends on the permittivity and the conductivity of the materials and on the frequency of the source. However, both conductivity and, in particular, permittivity are themselves frequency-dependent in biological tissues. This phenomenon is known as dispersion. In muscle, the relative permittivity varies by several orders of magnitude over the frequency range of the transmembrane action potential, which contains frequency components of up to 10 000 Hz [19]. Conductivity can vary by over 100% [12].

The goal of this paper is to understand the effects of tissue permittivity and dispersion in EMG models. Specifically, the following three questions are addressed. First, how do tissue material properties affect the displacement current density, the conduction current density and the maximum electric potential? Second, what error do we incur when we ignore dispersive effects in the calculation of the electric potential and how will this error change if we also neglect capacitive effects? Third, how do frequency and muscle-fiber conduction velocity affect the electric potential when we consider permittivity and dispersion?

In this paper, we present a frequency-domain and a time-domain analysis based on the finite-element method (FEM). This paper is a further development of the ideas presented in [32]. A single frequency excitation and a propagating muscle-

fiber action potential have been simulated in biological tissue where both conductivity and permittivity are incorporated. As yet, we are not aware of any time-domain numerical methods that can handle dispersion with time steps on the order of tens of microseconds, necessary to simulate the propagating single muscle-fiber action potential. Therefore, a combined approach is employed whereby the results of the time-domain simulations are corrected for dispersion in the frequency domain. This technique substantially reduces the computational burden as compared with solutions carried out solely in the frequency domain.

II. THEORETICAL BACKGROUND

The fundamental difference between computational models in EMG studies stems from the governing equations used. A clear statement of the governing equations permits a correct interpretation of the results. They necessarily differ in the frequency domain and in the time domain, both are presented.

A. Frequency Domain

1) Governing Equation: The electric scalar potential φ obeys

$$\nabla \cdot [(\sigma + j\omega\varepsilon_0\varepsilon_r)\nabla\varphi] = 0 \tag{2}$$

where j denotes the imaginary unit, $\nabla\cdot$ and ∇ denote the divergence of a vector function and the gradient of a scalar function, respectively. Equation (2) follows directly from Maxwell's equation describing Ampere's law [17] by taking the divergence on both sides under the assumption of negligible magnetic effects (vanishing magnetic vector potential). For the problems at hand, this assumption can be readily justified [26], [20].

2) The Phase Distribution in the Frequency Domain: In addition to the amplitude of the signal, a frequency-domain model also yields its spatial phase distribution $\theta(x, y, z)$. In most circumstances, capacitive effects will cause nonconstant spatial phase distributions. However, they will yield a constant spatial phase distribution if the model has homogeneous material properties, only current excitations, and is grounded. This can be seen in the simple case of a cylinder with current flowing parallel to its axis (no variation in radial direction) and a ground at one end. The cylinder can be represented by a parallel circuit of a resistor R and a capacitor C. The phase angle between current and voltage at angular frequency ω is given by $\arctan(\omega RC)$. As the observation point moves along the axis, the resistance will change proportionally, and the capacitance will change inversely proportionally to the distance from the ground, thus maintaining a constant product. At each point, the phase angle between current and voltage will be exactly equal to the argument (polar angle) of the complex number $\sigma + j\omega\varepsilon_0\varepsilon_r$. Since there are no phase variations of the current (no propagation effects), there will be no phase variations of the voltage either.

B. Time Domain

1) Governing Equation: In the time domain, the governing equation for the electric scalar potential is the following:

$$\nabla \cdot \left[\left(\sigma + \varepsilon_0\varepsilon_r\frac{\partial}{\partial t}\right)\nabla\varphi\right] = 0. \tag{3}$$

For the derivation of (3), it is assumed that the magnetic vector potential vanishes, as it does in the frequency domain. It is also assumed that the relative permittivity does not change with time, i.e., $\varepsilon_r(t) = const$. If the scalar potential in (2) is regarded as a function of frequency, it is possible to view (2) as the Fourier transform of (3). In order to keep the notation simple, the same symbols will be used in the frequency domain and in the time domain, and it will be clear from the context which domain is meant.

2) Dispersion: One method of generalizing (3) to incorporate dispersive materials is to allow σ and ε_r to vary with frequency in (2). Then using the convolution theorem [21] and transforming (2) into the time domain, we obtain

$$\nabla \cdot \left[\int_{-\infty}^{+\infty} K(t-\tau)\nabla\varphi(\tau)\,d\tau\right] = 0. \tag{4}$$

The kernel $K(t)$ is the inverse Fourier transform of $\sigma(\omega) + j\omega\varepsilon_0\varepsilon_r(\omega)$ (provided it exists). It is independent of φ. Thus, the problem remains linear. The condition $K(t) = 0$ for $t < 0$ is imposed in order to preserve causality (otherwise the potential at some moment in time will depend on future values as seen from (4) for $\tau > t$) [17].

III. METHODS AND MODELS

In this section, we describe how the general concepts discussed in the previous section are applied so as to understand the influence of capacitance and dispersion on the EMG signal. The numerical and analytical procedures are outlined, and the specific models are introduced.

A. The finite-element Method

The commercial FEM software package EMAS by ANSOFT Corp. was used to develop the models. Its formulation is based on the time integral of the electric scalar potential in the time domain and on $\varphi/(j\omega)$ in the frequency domain. In both domains, the magnetic vector potential $\vec{A}$ is used as well. This formulation allows for the solution of the complete system of Maxwell's equations. The formulation imposes the Coulomb gauge, which confines all propagation effects exclusively to the magnetic vector potential [17]. Since our specific problem does not include propagation or any other effects involving the magnetic field, it is possible to discard the components of $\vec{A}$ from the stiffness matrix prior to decomposition. This increases the numerical efficiency of the solution substantially.

B. Geometry of the Models

In both the frequency and the time domain, the geometry of the model was chosen so as to resemble a segment of a human limb. The limb segment (volume conductor) had the shape of a circular cylinder. In the frequency domain, it had a radius of 5 cm and a length of 30 cm. The volume conductor was placed into a cylinder of air with a radius 7 cm and a length of 34 cm. The purpose of the air cylinder was to provide means for applying outer grid boundary conditions, which will be discussed below. In the time domain, the idealized limb segment had a radius of 4 cm and a length of 15 cm (Fig. 1). The smaller size, while still realistic, allowed for reduction of the time and
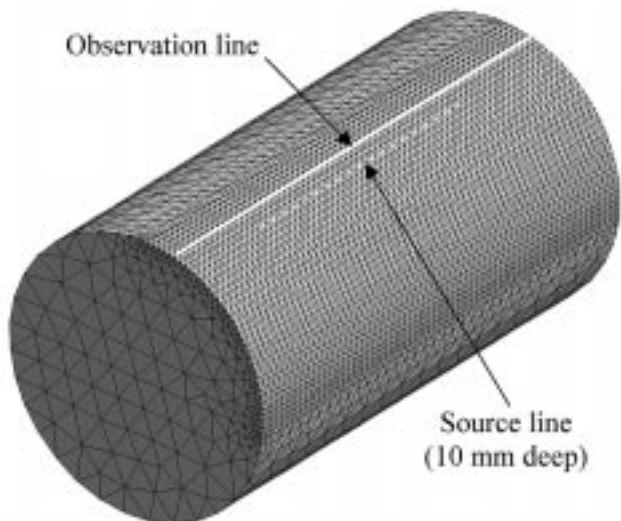
Fig. 1. The discretized time-domain FEM model. The radius is 4 cm and the length is 15 cm. The observation line is indicated. The 10-cm-long segment of an active muscle fiber is placed at 1 cm in radial direction from the observation line. Element size at the source is 0.1 mm, at the observation line 2 mm and up to 6 mm elsewhere.

resources needed to obtain the computationally more intense time-domain solution. For the same reason, this model did not include any surrounding air. However, the potential error due to the absence of air was assessed prior to the simulations and will be addressed in this section together with the outer grid boundary conditions.

C. Sources

1) Frequency Domain: The continuous source of the action potential is traditionally replaced by discrete sources like dipoles and tripoles [24]. A spatially fixed current dipole with pole separation of 2.1 mm and normalized source strength of 1 mA was simulated. This pole separation is equal to the distance between the centroids of the first positive and the following negative spatial wave in the single muscle-fiber action potential as analytically modeled by (5) and (6) according to Rosenfalk [31]. Thus, the first two spatial waves at a given moment in time were represented by the poles of the dipole placed at their centroids. The third spatial wave, which is much smaller than the first two, was neglected. This was possible because of the assumed linearity of the electrical properties of muscle. The dipole was spatially fixed, because frequency-domain analyses inherently presume a steady state of the system whereas a moving dipole gives rise to transient effects.

In frequency-domain analyses, it is assumed that all sources in the model have the same frequency which must be greater than zero. The physical meaning in the presented models is that each pole of the dipole is a source of alternating current of some frequency and there is a phase difference of $180°$ between them. There is an important difference between this dipole and a propagating but nonoscillating dipole (i.e., one whose poles are sources of direct current), as commonly used in EMG models [3], [10]. The spatially fixed current dipole gives rise to only one frequency throughout the model. It is the frequency at which the dipole is excited. A propagating dipole gives rise to a range of

frequencies and thus resembles a propagating action potential. However, it is essential to this study that we isolate single-frequency components of the field.

2) Time Domain: There were three sources in the model, which simulated the excitation of a 10-cm-long section of muscle fiber between the neuro-muscular junction and the tendon. The fiber was placed along a straight line parallel to the cylinder axis, symmetrically between the two ends of the cylinder at 10 mm below the surface. The first source represented the transmembrane current I during an action potential. It was propagating along the line of the muscle fiber according to the following spatio–temporal relationship [24], [31]:

$$I(\tilde{z}) = \begin{cases} S\sigma_i 96\tilde{z}\left(6 - 6\tilde{z} + \tilde{z}^2\right)e^{-\tilde{z}}, & \tilde{z} \geq 0 \\ 0, & \tilde{z} < 0 \end{cases} \quad (5)$$

$$\tilde{z} = t - z/v \quad (6)$$

where S denotes the average cross sectional area of the fiber and was chosen equal to 2.0×10^{-3} square millimeters (corresponding to a fiber diameter of 50 μm [19]), σ_i denotes the intracellular conductivity of the muscle fiber with a value 1.01 S/m [1], t denotes the time from the onset of the action potential in milliseconds, z denotes the distance of a point on the fiber from the neuro-muscular junction in millimeters, and v is the conduction velocity in millimeters per millisecond.

There were two more sources at both ends of the muscle fiber that simulated the start-up and end effects [7], [15], [9]. Their purpose was to ensure zero total current. At each moment in time, the source at the neuro-muscular junction yields a current equal in magnitude and opposite in sign to the net current of the propagating action potential. When the action potential reaches the end of the muscle fiber, the net current is calculated as if the fiber was infinite. The source at the other end yields a current equal to the part of the action potential which would extend beyond the end of the fiber, if the fiber were infinite. Therefore, it becomes active only after the action potential reaches the end. By that time the first source has become almost inactive, since the integral of the transmembrane current [as modeled by (5)–(6) over a sufficiently long segment of the fiber] is close to zero.

D. Outer Grid Boundary Conditions

Electric fields extend through air and free space to infinity by means of permittivity. A FEM mesh can have only finite dimensions. This difficulty, which does not arise in purely resistive models, requires special attention to the way a model with capacitive effects is terminated. EMAS provides a boundary condition that simulates open space at the outer boundary of the model, called spherical open boundary (SOB) [4]. As suggested by the name, it can be applied in three-dimensional models to patches of a sphere only, and as a result, the volume conductor must be embedded in a ball of air.

SOB is based on the Bayliss–Turkel approximation, expressed in a spherical coordinate system with origin in the center of SOB [34]

$$\frac{1}{c}\frac{\partial \varphi}{\partial t} + \frac{\partial \varphi}{\partial r} + \frac{1}{r}\varphi = 0$$

where $c = 2.997\,924\,58 \times 10^8$ m/s [17] denotes the speed of light in vacuum. The first term on the left-hand side can safely be neglected, and the first-order Bayliss–Turkel approximation reduces to [4]

$$\frac{\partial \varphi}{\partial r} + \frac{1}{r}\, \varphi = 0.$$

An unreasonably large number of elements are required to model the surrounding air, if the object of interest is a cylinder with a small ratio of radius to length of the axis. Our numerical experiments have shown that, in the frequency range of the EMG, using material properties of human tissues allows for the termination of the model by putting a ground on a surface sufficiently far (e.g., 2 cm) from the object of interest. The difference, as compared with a model with SOB, was 2.1% [20]. By further numerical simulation, we confirmed that excluding the surrounding air from the model as proposed in [26], yielded an almost identical result to that obtained with grounded 2-cm air layer (difference less than 0.5%). Furthermore, this generated a vanishing normal component of the electric field on the surface of the limb.

E. Ground Reference

It is useful to distinguish between physical and numerical ground reference.

1) Physical Ground Reference: A physical ground reference can occur as a part of Dirichlet or mixed boundary conditions. It can extend over patches of surfaces. Its presence affects the structure of the field, usually by "bending" it locally. The current flowing through the patch will be different with or without the ground—the physical ground is a current carrying ground reference.

A physical ground reference was used only in the frequency-domain analysis. It was applied to all surfaces of the air cylinder to provide outer grid boundary conditions as discussed in the previous section. Since the frequency-domain models with the supplied excitations and boundary conditions proved electrically symmetric about the transversal plane of geometric symmetry, a physical ground reference was applied to this plane as well, and only one half of the model was numerically processed.

2) Numerical Ground Reference: A numerical ground reference occurs only together with Neumann boundary conditions. The Neumann boundary condition determines the solution of the boundary-value problem only up to an additive constant [22]. To eliminate this ambiguity, it is sufficient to provide a ground reference at only one point in the model. The structure of the field will be preserved. The current density at that point will be the same with and without the ground—the numerical ground is not a current carrying ground reference. On the other hand, specifying ground over a patch of surface will change the nature of the boundary conditions and the structure of the field (the field will be "flattened"). Therefore, this kind of ground reference can be applied only to one single point in the model. It is important that the sum of all enforced currents in the model be zero, as dictated by the Neumann boundary conditions.

A numerical ground was used only in the time-domain analysis. It was applied to a point as far away from the source as possible. The distance from the source was considered in order

to minimize adverse effects due to unbalanced currents as a result of round-off errors.

F. Initial Conditions

The initial conditions are only applicable to problems in the time domain. The initial value of the scalar potential was zero throughout the model.

G. Convergence and Validity

FEM yields only an approximation to the true solution. Two methods for increasing the accuracy of the approximation are available, reducing the maximum diameter of the elements, and/or increasing the degree of the polynomials in the shape functions. However, there are instances in which increasing the degree of the polynomials does not ensure convergence [36]. We confirmed convergence by decreasing the element size. Increasing the number of elements up to six times the initial value produced a deviation of less than 3%.

While convergence indicates self-consistency of the model, it implies nothing about its ability to reflect the physical reality adequately. In a previous work [20], we validated our FEM technique by comparing simulated data with measured potentials in a physical phantom limb model. The numerical and the experimental data were highly correlated (the correlation coefficient was greater than 0.99) and absolute differences were generally within 5%–10%. However, the validity of the method was proved under nondispersive conditions.

H. Analytical Methods for Handling Dispersion

Since the available implementation of the FEM does not handle dispersion, additional tools were necessary in the study. The analytical approach described here in combination with the finite-element models provided a simple means by which to solve the dispersive field problems encountered in this study.

1) Dispersion Error in the Frequency Domain: For a homogeneous, isotropic volume conductor (capacitive effects included), we define $\kappa(\omega, \omega_m)$ as follows:

$$\kappa(\omega, \omega_m) = |\sigma(\omega_m) + j\omega\varepsilon(\omega_m)| \qquad (7)$$

where ω is the angular frequency of the source and ω_m is the angular frequency which was used in the parametric models [13] to calculate the material properties. Then the relative error $\delta(\omega, \omega_m)$ of the voltage amplitude at angular frequency ω due to using material properties at angular frequency ω_m is given by

$$\delta(\omega, \omega_m) = \frac{\kappa(\omega, \omega) - \kappa(\omega, \omega_m)}{\kappa(\omega, \omega_m)}. \qquad (8)$$

This error is independent of the spatial coordinates.

2) Dispersion in the Time Domain: The linearity of the problem (i.e., validity of the superposition principle) and the availability of precise expressions for the dispersion error in the frequency domain suggest a straightforward procedure to obtain an exact solution of the dispersive field problem in the time domain. This indirect method consists of calculating the Fourier transform of the available time-domain solution for a given set of nondispersive dielectric material properties, modifying it to account for the dispersion error in the frequency domain and transforming it back into the time domain. Because

TABLE I
RATIO OF DISPLACEMENT TO CONDUCTION CURRENT DENSITY (%) FOR DIFFERENT MATERIAL PROPERTIES.
THE RANGE OF REPORTED MATERIAL PROPERTIES [11]–[13] AT 100 Hz WAS USED

Conductivity	Displacement over conduction current density (%) at 100 Hz			
(S/m)	Static model	$\varepsilon_r=3.0\times10^5$	$\varepsilon_r=3.7\times10^6$	$\varepsilon_r=2.0\times10^7$
$\sigma=0.07$	0	2.4	29.4	159.0
$\sigma=0.24$	0	0.7	8.4	45.3
$\sigma=0.60$	0	0.3	3.4	18.5

TABLE II
THE MAXIMUM SURFACE POTENTIAL (MILLIVOLTS) AT 100 Hz FOR DIFFERENT MATERIAL PROPERTIES.
THE RANGE OF REPORTED MATERIAL PROPERTIES OF MUSCLE [12], [13] AT 100 Hz WAS USED

Conductivity	Maximum surface potential in (mV)			
(S/m)	Static model	$\varepsilon_r=3.0\times10^5$	$\varepsilon_r=3.7\times10^6$	$\varepsilon_r=2.0\times10^7$
$\sigma=0.07$	18.6	18.6	17.8	9.9
$\sigma=0.24$	5.3	5.3	5.3	4.8
$\sigma=0.60$	2.2	2.2	2.2	2.2

of the linearity of the problem, the inverse Fourier transformation yields the correct solution for the set of dispersive material properties. The correction can be performed as follows:

$$\varphi_2(\omega) = \varphi_1(\omega)p_1/p_2(\omega). \tag{9}$$

φ_1 is the Fourier transform of the available time-domain solution calculated for the set of nondispersive material properties σ_1 and ε_{r1}, φ_2 is the Fourier transform of the new solution for the set of dispersive material properties $\sigma_2(\omega)$ and $\varepsilon_{r2}(\omega)$, and $p_k = \sigma_k + j\omega\varepsilon_0\varepsilon_{rk}$ for $k = 1, 2$.

IV. FREQUENCY DOMAIN MODELING RESULTS

A. Effect of Material Properties

To study the effect of material properties in frequency domain,[1] we chose a frequency of 100 Hz. This is in the range of clinically observed mean frequency of surface EMG (68–129 Hz) [23]. A broad range of conductivities (0.070–0.600 S/m) and corresponding relative permittivities ($3 \times 10^5 - 2 \times 10^7$) have been reported for mammalian skeletal muscle and are reviewed in [11] and [12]. We calculated the correlation coefficient between σ and ε_r at 100 Hz, assuming that each pair of reported values was a pair of corresponding observations of the two variables. The obtained value of 0.09 indicated that any combination of conductivity and permittivity within their respective range of variation might possibly occur.

The full range of reported conductivities combined with the full range of reported permittivities was used to perform the analyses. For comparison, the static model (purely resistive case) was also simulated. Parametric Cole–Cole type of bio-electric models proposed by Gabriel *et al.* [13] were used to obtain values of conductivity and relative permittivity that lie within the middle of the range of experimentally measured data (0.24 S/m and 3.7×10^6, respectively). Table I shows the ratio of displacement current density to conduction current density. The smallest nonzero value occurs with the highest conductivity and the lowest permittivity, and the highest value occurs at the opposite ends of the ranges. Significant displacement currents are seen with several combinations. In the most extreme case, with the lowest conductivity and highest permittivity, the displacement current is larger than the conduction current.

The effect of these displacement currents on the electric potential at the surface is shown in Table II. Displacement currents resulted in a decrease of the surface potential with the higher permittivity values. When the material properties of muscle at 100 Hz given by [11], [12] are used, the range of relative error due to neglecting capacitive effects is between 0% and 88%. Using the mid-range values of conductivity and relative permittivity, we found that the difference between purely resistive models and models that include displacement currents was

---

[1] The frequency-domain analysis is based on "A finite-element analysis of muscle tissue capacitive effects and dispersion in EMG" by N. S. Stoykov, M. M. Lowery, A. Taflove, T. A. Kuiken which appeared in the *Proceedings of the 23rd Annual International Conference of IEEE Engineering in Medicine and Biology Society*, Istanbul, Turkey, Oct. 2001. © 2001 IEEE.
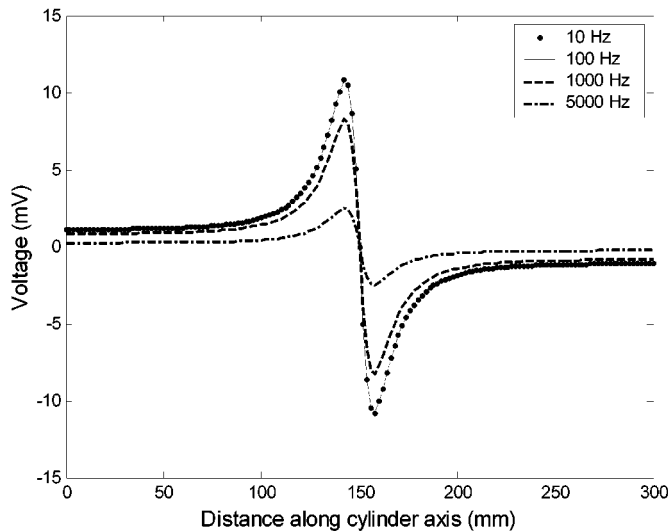
Fig. 2. Surface voltage along a line above the source parallel to the cylinder axis in a frequency-domain model. Conductivity and permittivity at 100 Hz were used for four different frequencies of the source, as displayed in the legend.

Fig. 3. The relative error in electric potential due to exclusion of dispersion is plotted as a function of frequency for different tissues. The error is incurred if values for conductivity and permittivity at 100 Hz are used at other frequencies.

within the range of the convergence error of the models (i.e., less than 3%). The variation in conductivity clearly has a larger effect on the surface potential. The maximum surface potential decreases with increasing conductivity.

B. Effect of Dispersion

EMG frequency content near the source is high—the median frequency for single-fiber EMG is 1610 ± 300 Hz [19]. Spatial filtering rapidly lowers the frequency content so that the mean frequency at the surface is near 100 Hz [23], [24]. The tissues in the arm are, therefore, exposed to a wide range of frequencies.

Source frequencies of 10, 50, 200, 1000, 1500, and 5000 Hz were used to assess the error at a single frequency due to neglecting dispersive effects. This range includes frequencies observed near the surface as well as near the source. The relative error incurred if the frequency-dependent values of conductivity and relative permittivity were replaced by the values at 100 Hz was calculated. Material properties were obtained from the parametric models in [13]. The error at 10, 1000, and 5000 Hz was calculated both by FEM and by the analytical expressions (7)–(8). FEM was used to obtain the error at the site of maximum surface potential (Fig. 2). Within three decimal places, (7)–(8) yielded the same results. For the remaining frequencies, the error was calculated only by using (7)–(8). Table III summarizes the relative error at each frequency with and without displacement currents included. Fig. 3 shows the frequency behavior of the error over a range from 0 to 5000 Hz for muscle and several other tissues. Displacement currents were included. Equations (7)–(8) were used to obtain the data.

C. Effect of Frequency

The effect of frequency on the maximum surface potential was studied with a 1 mA input current. Source frequencies of 10, 100, 1000, and 5000 Hz were used. At each frequency, mid-range material properties were obtained from the parametric models presented in [13] and assigned to the model. The
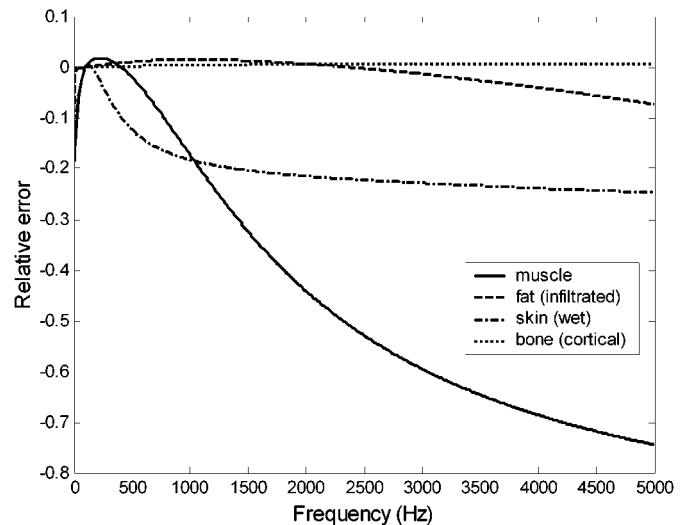
maximum surface potentials for different simulation conditions are presented in Table IV. There is a relatively large difference (33%) between the low and the high end of the spectrum. Most of this difference occurs between 10 and 100 Hz, at the low end of the spectrum. There is practically no difference between the results calculated with or without capacitive effects considered when material properties obtained from the parametric models [13] are used.

V. TIME–DOMAIN MODELING RESULTS

A. Effect of Material Properties

While the frequency-domain analysis presented in Section IV-A shows the sensitivity of the maximum surface potential to variations in the dielectric properties at one frequency, it remains unclear how this variation would affect the compound field due to a propagating single muscle-fiber action potential. To answer this question, a mid-range muscle conductivity of 0.24 S/m (as obtained from the parametric models [13] at frequency of 100 Hz) was used in the time-domain model. The relative permittivity of muscle was varied as in the frequency-domain study. The muscle-fiber conduction velocity was assumed to be 4 m/s. The results indicate a decrease of amplitude with increasing permittivity [Fig. 4(A)]. The decrease follows a nonlinear relationship, resembling the corresponding result in the frequency domain. A change in the shape of the signal is also apparent. This is confirmed by a spectral analysis of the signal [Fig. 4(B)]. While the spectral components below 50 Hz remain unchanged in all three simulations, those above 50 Hz are notably attenuated for $\varepsilon_r = 2.0 \times 10^7$. As a result the median frequency has decreased from 133 to 122 Hz.

To prove numerical consistency between the FEM model and the analytical approach in the time domain, both were used to calculate the solution along a line on the surface of the model, 7.5 ms after onset of the action potential. The line was oriented in axial direction and was located just above the source (Fig. 1). Mid-range material properties of $\sigma = 0.24$ S/m and $\varepsilon_r = 2.0 \times$

TABLE III
THE RELATIVE ERROR (%) OF THE SURFACE POTENTIAL WHEN THE MATERIAL PROPERTIES
AT 100 Hz ARE USED AT OTHER FREQUENCIES

Type of solver	Relative error (%)					
	10 Hz	50 Hz	200 Hz	1000 Hz	1500 Hz	5000 Hz
Including Displacement Currents $\sigma=0.24$ S/m $\varepsilon_r=3.7\times10^7$	−16.8	−4.5	1.8	−17.3	−32.4	−74.4
Excluding Displacement Currents $\sigma=0.24$ S/m	−16.8	−4.4	3.2	7.9	8.6	10.2

TABLE IV
EFFECT OF FREQUENCY ON MAXIMUM SURFACE POTENTIAL WITH A 1 mA INPUT CURRENT. THE CORRECT
MATERIAL PROPERTIES OF MUSCLE AS OBTAINED BY A PARAMETRIC MODEL [13] WERE USED

Type of solver	Maximum surface potential in (mV)			
	10 Hz	100 Hz	1000 Hz	5000 Hz
Displacement Currents	6.5	5.4[a]	5.0	4.9
No Displacement Currents	6.5	5.4[a]	5.0	4.9

[a]: The difference of 1.9% is due to different FEM meshes of the same model (see Table II).
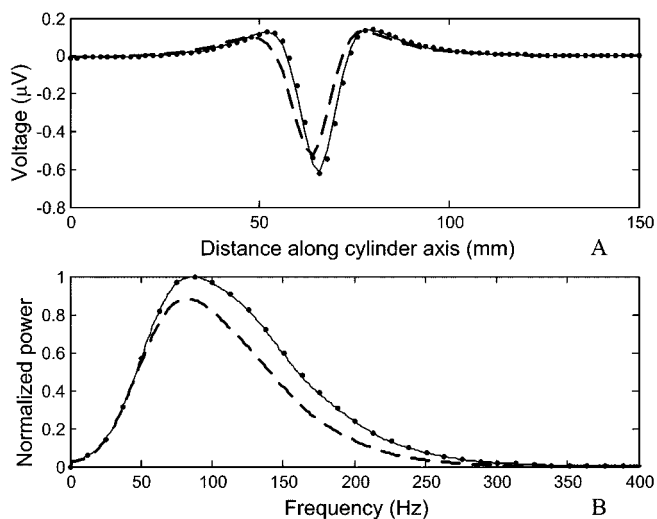
Fig. 4. (A): The surface voltages along an observation line above the source with different permittivities (dashed line, $\varepsilon_r = 2.0 \times 10^7$; solid line, $\varepsilon_r = 3.7 \times 10^6$; dotted line, static model). The results at 7.5 ms after the onset of the action potential are plotted. $\sigma = 0.24$ S/m, conduction velocity =4 m/s. (B): Corresponding normalized power spectrum, with notable attenuation of the signal components above 50 Hz.

10^7 were used. At each point of the line, the difference between the analytical solution and the FEM solution was less than 1.8% of the range of the signal.

B. Effect of Dispersion

Fig. 3 suggests that larger effects of dispersion in muscle should be expected at frequencies above 500 Hz. Since the mean frequency of the EMG signal decreases with increasing distance from the source [24], [23], these effects should be more pronounced close to the source. Therefore, the recording site in this simulation was chosen at 200 μm from the fiber. Conduction velocity of 4 m/s was used. First, the nondispersive solution was calculated by the FEM model. Mid-range values for conductivity and relative permittivity at 100 Hz were used (0.24 S/m and 3.7 × 10^6). The dispersive solution was then calculated by the analytical approach for material properties obtained from the parametric models [13]. The results are presented in Fig. 5. Neglecting dispersion caused 8.5% decrease in the peak-to-peak amplitude of the signal. The median frequency decreased from 571 Hz when dispersion was included, to 514 Hz when dispersion was neglected.

C. Effect of Conduction Velocity

The effect of conduction velocity on the EMG signal under dispersive conditions was examined by the analytical approach in two steps. In the first step, mid-range material properties of muscle at 100 Hz ($\sigma = 0.24$ S/m, $\varepsilon_r = 3.7 \times 10^6$) as obtained from the parametric models in [13] were used to calculate the nondispersive time-domain solution for conduction velocities of 3, 4, and 5 m/s [19]. In the second step, the time-domain results were corrected to allow for dispersion.

The surface voltage distribution along the line parallel to the cylinder axis and immediately above the source (Fig. 1) was compared for the three conduction velocities. Observations were taken at 10, 7.5, and 6 ms after onset of the action potential for conduction velocity of 3, 4, and 5 m/s, respectively. By then, the start-up effects had died away, and the front of the propagating action potential was 30 mm from the neuromuscular junction. At no point along the observation line did the
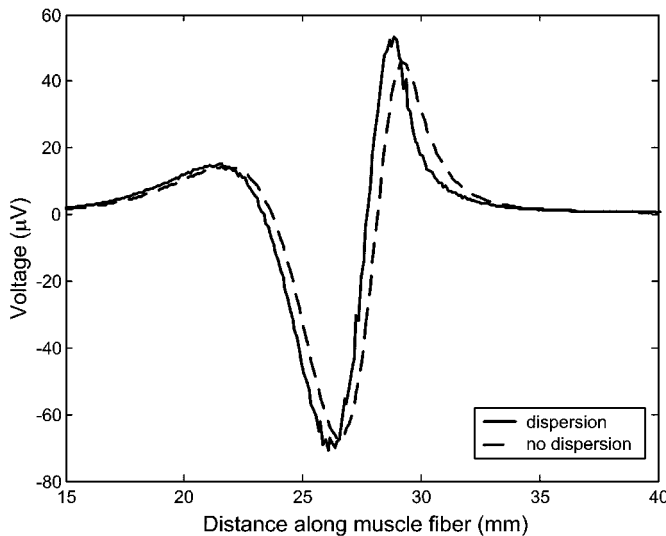
Fig. 5. Potential calculated along a line parallel to the muscle fiber 200 μm from it for an action potential propagating at 4 m/s to the right with and without dispersion. When dispersion is accounted for, the whole dispersion curve is used to obtain the correct material properties. When dispersion is neglected, only material properties at 100 Hz are used.

absolute difference between the voltage at the highest and the lowest conduction velocity exceed 5.9% of the peak-to-peak amplitude. The differences for the other combinations of conduction velocities were smaller.

VI. DISCUSSION

In this paper, capacitive effects, dispersion of conductivity and dispersion of permittivity in muscle are examined in the frequency domain and in the time domain. An oscillating dipole is proposed as a single-frequency source in the frequency domain. A realistic propagating single-fiber action potential is the source used in the time domain.

The magnitude of the capacitive and dispersive effects in the simulated EMG signal depends on the material properties, the frequency content of the source, and the muscle-fiber conduction velocity. Therefore, all numerical experiments were designed so as to cover the essential range of these parameters. The frequency-domain models provide information about the effects under study at the level of a single frequency component of the signal. Alternatively, the time-domain models address the effects at the level of the compound signal.

The analysis of the effects of material properties on the ratio of displacement to conduction-current density and on the maximum surface potential incorporates variation in the material properties across several animal species. It is suggested in [12], that the differences between human and animal species are not systematic, and that differences within a species may exceed differences across species. As stated in [11], the reported values of material properties were measured under varying conditions regarding temperature and freshness of the samples. It is also not clear how different physiological conditions affecting the electrolyte balance (e.g., during hemodialysis) might influence the material properties. Under these restrictions, the results show

that capacitive effects can give rise to a significant level of displacement-current densities relative to the conduction-current density, which results in a decrease of the maximum surface potential (Tables I and II). Apparently, displacement currents provide an additional pathway for the flow of energy through the limb, thus reducing the impedance of the limb. Consistent with this notion are the time-domain results presented in Fig. 4. They establish that capacitive effects have the nature of a low-pass filter and depend nonlinearly on material properties. Both the frequency-domain and the time-domain results show that capacitive effects are negligible for mid-range material properties.

A very important aspect of the frequency-domain analysis of dispersion is the choice of frequency range. As stated in Section IV-B above, the tissues in the limb are exposed to a wide range of frequencies. An example of the high end of this range is given by the model source (5)–(6). 20% of its integrated amplitude spectrum at 5 m/s lies above 5000 Hz. The whole range, therefore, must be considered when simultaneous observations are taken throughout the volume conductor [30], even though the high-end frequencies are not representative of the frequency content of signals recorded far away from the source.

The dispersion error was calculated in the frequency domain at the site of maximum surface potential. This site does not change for different material properties as long as the limb remains homogeneous (Fig. 2), because in this case, material properties have only a scaling effect on the potential distribution. Furthermore, the error is the same throughout the volume conductor due to the constant current excitation.

Dispersion can have a dramatic effect on the fields calculated at a single frequency. It is much more pronounced when displacement currents are included than in purely resistive models. For frequencies below that at which material properties are being used, the static solver (without displacement currents) underestimates the voltage. For frequencies above it, the voltage is overestimated (Table III). No general trend exists if displacement currents are included (Table III and Fig. 3).

An explanation of this behavior is found in the frequency dependence of conductivity and permittivity. The conductivity is an increasing function of frequency. Thus, at lower frequencies it will be overestimated and the voltage—according to Ohm's law—underestimated. The high frequency behavior can be explained accordingly. Unlike conductivity, permittivity is a decreasing function of frequency. However, not permittivity alone, but rather the product of permittivity and angular frequency determines the effect of displacement currents, as it can be recognized in (1). Whether the voltage will be overestimated or underestimated depends on the complex relationship between conductivity and permittivity given by (7)–(8).

The analysis of the effect of frequency on the EMG signal can be viewed as characterizing the transfer function between the source and the observation point. Permittivity has practically no effect when the mid-range values of ε_r are used. The results in Table IV indicate that with mid-range dielectric constants, dispersion in the muscle conductivity has a more pronounced effect than permittivity, especially at lower frequencies. Changes in conduction velocity directly translate into changes of the frequency content of the source by the scaling property of the Fourier transformation [21]. In the time domain, the analysis

of the effect of conduction velocity on the signal shows that, for the dispersion curves of muscle provided by the parametric models in [13], conduction velocity has little effect on the amplitude of the surface EMG signal. A linear relationship between conduction velocity and muscle-fiber diameter has been used in EMG modeling [15]. This relationship was not included in the present analysis in order to obtain more transparent results. We are convinced that there is no loss of generality with respect to the question addressed here.

This study has been limited to muscle. However, most biological tissues have high permittivities and are highly dispersive. In particular, skin has relatively low conductivity and high permittivity so that capacitive as well as dispersive effects are expected to be significant. The proposed method for handling dispersion is applicable only to homogeneous models. If dispersion is to be included in an inhomogeneous model, the analysis must be done in the frequency domain. Alternatively, new time-domain Maxwell-equation solvers capable of handling dispersion must be developed to obtain temporal waveforms of propagating EMG signals directly. Using a single value of permittivity (from one frequency) can cause large errors in estimating signal content at the higher frequencies.

While the methods described may be applicable to problems in other areas of bioelectric research, the particular results will vary according to the different dispersion curves and the different frequency content of the sources.

VII. CONCLUSION

The results indicate that capacitive effects in muscle may vary from having a negligible influence on the simulated EMG signal to having a considerable impact, depending on the combination of electric conductivity and permittivity used. These effects should be considered with any bioelectromagnetic model. Whether or not they should be included depends on the particular model used in the investigation. For mid-range material properties of muscle, capacitive effects are small for frequencies between 10 and 5000 Hz. Since the reported range of conductivity and relative permittivity spreads over several orders of magnitude, even at a single frequency, it is important to identify their values correctly.

Dispersive effects in muscle can be important. Dispersion in muscle conductivity is significant and can cause an error of up to 33% in single frequency components of the signal. Most of the error occurs at lower frequencies where the fall-off of conductivity is faster. With errors as high as 74% at the high end of the spectrum, dispersion in permittivity can have a great impact on single-frequency components of the signal. As a result, the compound signal can be distorted, but to a much smaller degree. Changes of 8.5% in the peak-to-peak amplitude and of 10% in the median frequency of the power spectrum have been observed in the model.

Including capacitive effects in a model but neglecting their dispersive nature can cause a larger error than omitting them altogether. Consequently, further work toward developing dispersive solvers is indicated by this study.

REFERENCES

[1] S. Andreassen and A. Rosenfalck, "Relationship of intracellular and extracellular action potentials of skeletal muscle fibers," *CRC Crit. Rev. Bioeng.*, pp. 267–306, Nov. 1981.

[2] P. J. Basser, R. S. Wijesinghe, and B. J. Roth, "The activating function for magnetic stimulation derived from a three-dimensional volume conductor model," *IEEE Trans. Biomed. Eng.*, pp. 1207–1210, Nov. 1992.

[3] D. C. Boyd, P. D. Lawrence, and P. A. Bratty, "On modeling the single motor unit action potential," *IEEE Trans. Biomed. Eng.*, vol. BME–15, pp. 236–242, 1978.

[4] J. R. Brauer and B. S. Brown, Eds., *EMAS User's Manual—Version 4*. Pittsburgh, PA: Ansoft Corp., July 1997, pp. 72–76.

[5] M. A. Camacho, J. L. Lehr, and S. R. Eisenberg, "A three-dimensional finite element model of human transthoracic defibrillation: Paddle placement an size," *IEEE Trans. Biomed. Eng.*, pp. 572–578, June 1995.

[6] G. Cerri, R. De Leo, F. Moglie, and A. Schiavoni, "An accurate 3-D model for magnetic stimulation of the brain cortex," *J. Med. Eng. Tech.*, pp. 7–16, Jan./Feb. 1995.

[7] N. Dimitrova, "Model of the extracellular potential field of a single striated muscle fiber," *Electromyogr. Clin. Neurophysiol.*, vol. 14, pp. 53–66, 1974.

[8] P. M. Edic, G. J. Saulnier, J. C. Newell, and D. Isaacson, "A real-time electrical impedance tomograph," *IEEE Trans. Biomed. Eng.*, pp. 849–859, Sept. 1995.

[9] D. Farina and R. Merletti, "A novel approach for precise simulation of the EMG signal detected by surface electrodes," *IEEE Trans. Biomed. Eng.*, vol. 48, pp. 637–646, June 2001.

[10] A. J. Fuglevand, D. A. Winter, A. E. Patla, and D. Stashuk, "Detection of motor unit action potentials with surface electrodes: Influence of electrode size and spacing," *Biol. Cybern.*, vol. 67, pp. 143–153, 1992.

[11] C. Gabriel, S. Gabriel, and E. Corthout, "The dielectric properties of biological tissues: I. Literature survey," *Phys. Med. Biol.*, vol. 41, pp. 2251–2269, 1996.

[12] S. Gabriel, R. W. Lau, and C. Gabriel, "The dielectric properties of biological tissues: II. Measurements in the frequency range 10 Hz to 20 GHz," *Phys. Med. Biol.*, vol. 41, pp. 2251–2269, 1996.

[13] ——, "The dielectric properties of biological tissues: III. Parametric models for the dielectric spectrum of tissues," *Phys. Med. Biol.*, vol. 41, pp. 2271–2293, 1996.

[14] F. L. Gielen, W. Wallinga-de Jonge, and K. L. Boom, "Electrical conductivity of skeletal muscle tissue: Experimental results from different muscles *in vivo*," *Med. Biol. Eng. Comput.*, vol. 22, pp. 569–577, 1984.

[15] T. H. J. M. Gootzen, D. F. Stegeman, and A. Van Oosterom, "Finite limb dimensions and finite muscle length in a model for the generation of electromyographic signals," *Electroencephalogr. Clin. Neurophysiol.*, vol. 81, pp. 152–162, 1991.

[16] H. Griffiths, "Tissue spectroscopy with electrical impedance tomography: Computer simulations," *IEEE Trans. Biomed. Eng.*, pp. 948–954, Sept. 1995.

[17] J. D. Jackson, *Classical Electrodynamics*, 3rd ed. New York: Wiley, 1999, pp. 238–242, 330–333, 782.

[18] D. B. Jorgenson, P. H. Schimpf, I. Shen, G. Johnson, G. H. Bardy, D. R. Haynor, and Y. Kim, "Predicting cardiothoracic voltages during high energy shocks: Methodology and comparison of experimental to finite element model data," *IEEE Trans. Biomed. Eng.*, pp. 559–571, June 1995.

[19] J. Kimura, *Electrodiagnosis in Diseases of Nerve and Muscle: Principles and Practice*, 2nd ed. Philadelphia, PA: Davis, 1989, p. 212, 230, 290.

[20] T. Kuiken, N. Stoykov, M. Popovic, M. Lowery, and A. Taflove, "Finite element modeling of electromagnetic signal propagation in a phantom arm," *IEEE Trans. Neural Syst. Rehab. Eng.*, vol. 9, pp. 346–354, Dec. 2001.

[21] S. L. Marple, Jr., *Digital Spectral Analysis*. Englewood Cliffs, NJ: Prentice-Hall, 1987, p. 32.

[22] V. N. Maslennikova, *Partial Differential Equations*. Moscow, Russia: RUDN, 1997.

[23] R. Merletti and L. R. Lo Conte, "Surface EMG signal processing during isometric contractions," *J. Electromyogr. Kinesiol.*, vol. 7, pp. 241–250, 1997.

[24] R. Plonsey, "The active fiber in a volume conductor," *IEEE Trans. Biomed. Eng.*, pp. 371–381, Sept. 1974.

[25] R. Plonsey and R. C. Barr, "Electric field stimulation of excitable tissue," *IEEE Trans. Biomed. Eng.*, pp. 329–336, Apr. 1995.

[26] R. Plonsey and D. B. Heppner, "Considerations of quasistationarity in electrophysiological systems," *Bull. Math. Biophys.*, vol. 29, pp. 657–664, 1967.

[27] F. Rattay, "Analysis of models for external stimulation of axons," *IEEE Trans. Biomed. Eng.*, vol. BME-33, pp. 974–977, 1986.

[28] ——, "Ways to approximate current-distance relations for electrically stimulated fibers," *J. Theor. Biol.*, pp. 339–349, 1987.

[29] ——, "Modeling the excitation of fibers under surface electrodes," *IEEE Trans. Biomed. Eng.*, pp. 199–202, Mar. 1988.

[30] K. Roeleveld, D. F. Stegeman, H. M. Vingerhoets, and A. van Oosterom, "Motor unit potential contribution to surface electromyography," *Acta Physiol. Scand.*, vol. 160, pp. 175–183, 1997.

[31] P. Rosenfalck, "Intra- and extracellular potential fields of active nerve and muscle fibers. A physico-mathematical analysis of different models," *Acta Physiol. Scand.*, p. 60, 1969.

[32] N. S. Stoykov, M. M. Lowery, A. Taflove, and T. A. Kuiken. A finite element analysis of muscle tissue capacitive effects and dispersion in EMG. presented at Proc. 23rd Annu. Int. Conf. IEEE Engineering in Medicine and Biology Society, Oct. 2001. [CD-ROM]

[33] D. M. Sullivan, O. P. Gandhi, and A. Taflove, "Use of the finite-difference time-domain method for calculating EM absoption in man models," *IEEE Trans. Biomed. Eng.*, pp. 179–186, Mar. 1988.

[34] A. Taflove and S. Hagness, *Computational Electrodynamics: The Finite-Difference Time-Domain Method*, 2nd ed. Boston, MA: Artech House, 2000, pp. 237–243.

[35] B. K. van Veen, W. L. C. Rutten, and W. Wallinga, "Influence of a frequency-dependent medium around a network model, used for the simulation of single-fiber action potentials," *Med. Biol. Eng. Comput.*, vol. 28, pp. 492–497, 1990.

[36] O. C. Zienkiewicz and A. Craig, "Adaptive refinement, error estimates, multigrid solution, and hierarchic finite element method concepts," in *Accuracy Estimates and Adaptive Refinements in Finite Element Computations*, I. Babuska, O. C. Zienkiewicz, J. Gago, and E. R. de A. Olivera, Eds. Chichester, U.K.: Wiley, 1986, pp. 25–59.

Nikolay S. Stoykov (M'00) received the M.S. and Ph.D. degrees in biomedical engineering from the Technical University Ilmenau, Ilmenau, Germany, in 1990 and 1998, respectively.

Since 1999, he has been a Post-doctoral Fellow with the Department of Research, Rehabilitation Institute of Chicago, Chicago, IL, and with the Department of Physical Medicine and Rehabilitation, Northwestern University, Chicago. His research interests have focused on modeling bioelectric phenomena with the finite-element method.

Madeleine M. Lowery (M'00) received the B.E. and Ph.D. degrees from the Department of Electronic and Electrical Engineering, University College Dublin, National University of Ireland, Dublin, Ireland, in 1996 and 2000, respectively.

She is currently a Post-Doctoral Research Fellow with the Department of Physical Medicine and Rehabilitation in Northwestern University at the Rehabilitation Institute of Chicago, Chicago, IL. Her research interests include mathematical modeling and analysis of bioelectric signals, in particular surface EMG.

Allen Taflove (M'75–SM'84–F'90) was born in Chicago, IL on June 14, 1949. He received the B.S., M.S., and Ph.D. degrees in electrical engineering from Northwestern University, Evanston, IL in 1971, 1972, and 1975, respectively.

After nine years as a Research Engineer at the IIT Research Institute, Chicago, IL, he returned to Northwestern in 1984. Since 1988, he has been a Professor in the Department of Electrical and Computer Engineering of the McCormick School of Engineering. Currently, he is a Charles Deering McCormick Professor of Teaching Excellence and Master of the Lindgren Residential College of Science and Engineering. Since 1972, he has pioneered basic theoretical approaches and engineering applications of finite-difference time-domain (FDTD) computational electromagnetics. He coined the FDTD acronym in a 1980 IEEE paper, and in 1990 was the first person to be named a Fellow of IEEE in the FDTD area. He authored *Computational Electrodynamics—The Finite-Difference Time-Domain Method* (Norwood, MA: Artech House, In 1995). This book is now in its second edition, co-authored with Prof. Susan Hagness of the University of Wisconsin–Madison. He was the editor of the research monograph, *Advances in Computational Electrodynamics—The Finite-Difference Time-Domain Method* (Norwood, MA: Artech House, In 1998). In addition to the above books, he has authored or co-authored 12 invited book chapters, 73 journal papers, approximately 200 conference papers and abstracts, and 13 U.S. patents. He has been the thesis adviser of 14 Ph.D. degree recipients who hold professorial, research, or engineering positions at major institutions including the University of Wisconsin–Madison, the University of Colorado–Boulder, McGill University, Lincoln Lab, the Jet Propulsion Lab, and the U.S. Air Force Research Lab. Currently, he is conducting research in a wide range of computational electromagnetics modeling problems including the propagation of bioelectric signals within the human body, laser-beam propagation within samples of human blood, UHF diffraction by buildings in urban wireless microcells, microwave cavity resonances in subatomic particle accelerators, electrodynamics of micron-scale optical devices, novel wireless interconnects for ultrahigh-speed digital data buses, and ELF geophysical phenomena.

Todd A. Kuiken (M'99) received the Ph.D. degree in biomedical engineering and the M.D. degree from Northwestern University, Evanston, IL, in 1989 and 1990, respectively.

He was trained in physical medicine and rehabilitation at the Rehabilitation Institute of Chicago, Chicago, IL. He is currently Chief-of-Staff and the Director of Amputee Services at the Rehabilitation Institute of Chicago. He is an Assistant Professor in the Department of PM&R and the Electrical and Computer Engineering Department of Northwestern University. His research interests include the care of amputees, the control of artificial limbs, and myoelectric signal analysis.

Dr. Kuiken is a board certified Physiatrist.